The Role of Water and Influence of the Hydrogen Bonding on the Self-Assembly Aggregation Induced Emission of an Anthracene-Guanidine-derivative

Pedro J. Pacheco-Liñán,[£, †] Cristina Martín,[£, #, ‡] Carlos Alonso-Moreno,[‡, ∞] Alberto Juan,[α, ¥] Daniel Hermida-Merino,[‖] Andrés Garzón-Ruíz,[†] José Albaladejo,[χ] Mark Van der Auweraer,[#] Boiko Cohen*[,§] and Iván Bravo*[,†, ‡]

[†] Departamento de Química Física. Facultad de Farmacia de Albacete, Universidad de Castilla-La Mancha, Albacete-02071, Spain.

[#] Molecular Imaging and Photonics, Department of Chemistry, Katholieke Universiteit Leuven, Celestijnenlaan 200F, 3001 Leuven, Belgium

[‡] Unidad de Medicina Molecular, Centro Regional de Investigaciones Biomédicas, Albacete, Spain

[∞] Departamento de Inorgánica, Orgánica y Bioquímica. Facultad de Farmacia de Albacete, UCLM, Albacete-02071, Spain

[α] Department of Biomolecular Nanotechnology, MESA+ Institute for Nanotechnology and TechMed Institute for Health and Biomedical Technologies, Faculty of Science and Technology, University of Twente, P.O. Box 217, 7500 AE, Enschede, The Netherlands

[¥] Department of Molecular NanoFabrication, MESA+ Institute for Nanotechnology, Faculty of Science and Technology, University of Twente, P.O. Box 217, 7500 AE, Enschede, The Netherlands

[‖] Netherlands Organization for Scientific Research, DUBBLE at the ESRF, 71 Avenue des Martyrs, CS40220, 38043 Grenoble, France

[χ] Instituto de Investigación en Combustión y Contaminación Atmosférica, Universidad de Castilla-La Mancha, Camino de Moledores s/n, Ciudad Real, 13071, Spain

[§] Departamento de Química Física, Facultad de Ciencias Ambientales y Bioquímica, and INAMOL, Universidad de Castilla-La Mancha, Avenida Carlos III, S/N, 45071 Toledo

Materials. Acetonitrile, tetrahydrofuran (THF), ethanol, *N*,*N'*-diisopropylcarbodiimide, amines, $ZnEt_2$ (1M solution in hexane), dichloromethane, toluene and trifluoroacetic acid were purchased from Sigma-Aldrich (Spain). Hexane, NaOH and HCl were provided from Labkem (Spain). Deuterated water was purchased from Sigma-Aldrich (Spain). The highest purity grade available was used. All aqueous solutions were prepared in Milli-Q water and filtered with 0.22 μm filters prior to use. The pH of the aqueous solutions was adjusted using NaOH or HCl. Stock solutions were kept at 4°C in the dark. Mass spectroscopic analyses were performed on a Advion expression CMS instrument (electron impact). Guanidine melting point (m.p.) were determined using a Gallenkamp m.p. apparatus.

Computational methodology. Calculations were performed with the Gaussian09 (revision D.01) program package.[1] The initial conformational analysis was carried out at the B3LYP/6-31G* level of theory while final geometries were optimized at the B3LYP/6-31+G* level. Vertical electronic transitions were computed at the time-dependent TD-DFT level for the solvated molecule within the Polarizable Continuum Model (PCM) methodology.[2,3]

DFT theoretical calculations were performed in order to provide an overall interpretation of the photophysical processes observed. Figure 1S show optimized geometries of the mono and deprotonated dimer. The protonation of both guanidine groups implies a conformational change in the structure, in which the anthracenes go from being T-shaped to a parallel arrangement. Obtaining an on-off system, where the protonation state entails passing from one very emitting dimer to another fluorescence quenched.

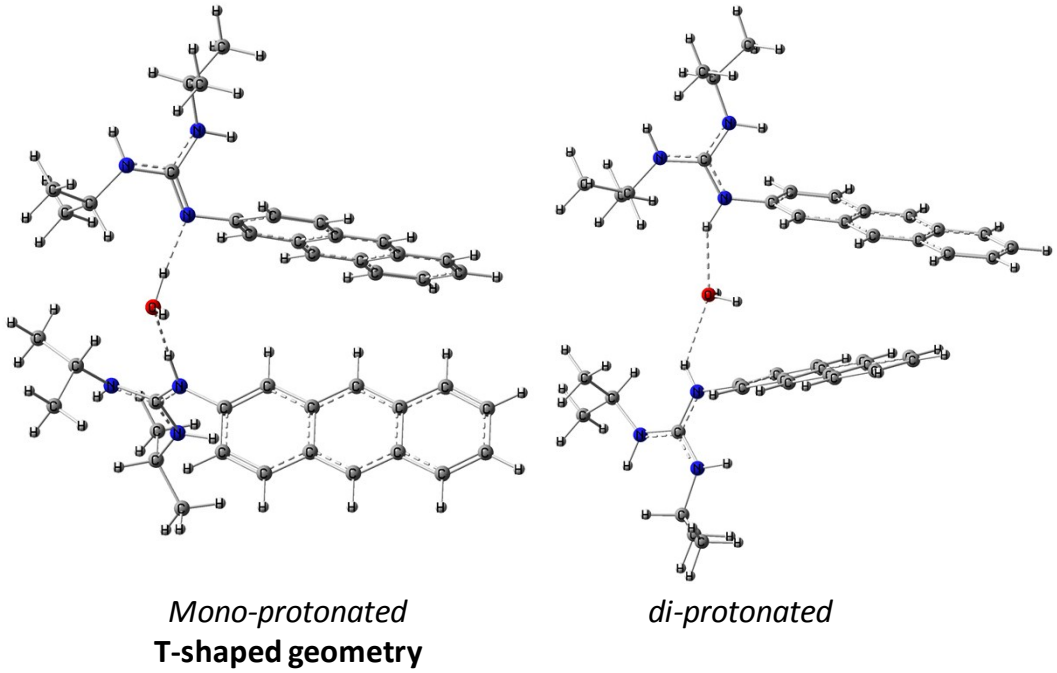

Figure 1S. Optimized geometries of the mono and di-protonated dimers

Table S1. Cartesian coordinates of optimized structures

T-shaped dimer				Parallel dimer			
C	-4.36604100	-1.72875300	-0.40506300	C	-4.90158200	0.68527700	-0.60622400
N	-4.47336700	-3.01981200	0.05016000	N	-5.55799100	-0.48067900	-0.57197300
H	-3.58663000	-3.43998000	0.29789900	H	-4.97951500	-1.30420900	-0.44827800
N	-5.53149200	-1.14308500	-0.82513500	N	-5.55634800	1.83270700	-0.84839500
H	-6.37887600	-1.59227500	-0.50389000	H	-6.55629900	1.76199100	-0.97824500
C	-5.55665000	-3.97472200	-0.23472300	C	-7.00760700	-0.70257500	-0.78996800
H	-6.50915000	-3.50275900	0.04440300	H	-7.53730500	0.11011200	-0.27495700
C	-5.67950100	0.28854200	-1.11492300	C	-5.01656200	3.20912000	-0.75565100
H	-4.77972600	0.59234000	-1.65375800	H	-4.02814800	3.20391000	-1.23336900
C	-5.78407300	1.12465900	0.16827700	C	-4.88473000	3.66417400	0.70331200
H	-4.90807100	0.96495700	0.80396900	H	-4.24540000	2.99065200	1.28320000
H	-5.84797300	2.19174100	-0.07384200	H	-4.45033700	4.66832500	0.74397400
H	-6.68113500	0.85627200	0.73998800	H	-5.86739900	3.70240000	1.18509600
C	-6.89384700	0.47682300	-2.02834800	C	-5.92731100	4.12696800	-1.57479500
H	-6.78577300	-0.10061500	-2.95179900	H	-5.98792500	3.80403200	-2.61865300
H	-7.81837800	0.15690900	-1.52972000	H	-6.94008000	4.15148400	-1.15397600
H	-7.01380900	1.53252100	-2.29203900	H	-5.54170600	5.14986200	-1.55479700
C	-5.61448100	-4.37418000	-1.71635800	C	-7.36196300	-0.69509700	-2.28293100
H	-5.73707500	-3.49543800	-2.35704500	H	-7.05884900	0.23527900	-2.77519300
H	-4.69251300	-4.88936500	-2.00993300	H	-6.87046800	-1.52622800	-2.79954000
H	-6.45578600	-5.05177400	-1.89933400	H	-8.44304000	-0.80801600	-2.41060300
C	-5.37061300	-5.18646900	0.68261400	C	-7.39400900	-2.01611400	-0.10626700
H	-5.35984300	-4.88644600	1.73514300	H	-7.16096700	-1.99466700	0.96273800
H	-6.18393500	-5.90290500	0.53453000	H	-8.46761100	-2.18947200	-0.21779700
H	-4.42880700	-5.70396700	0.45949600	H	-6.87338700	-2.86499400	-0.56607000
N	-3.23176400	-1.06736200	-0.42477800	N	-3.56613700	0.70201200	-0.38899600
C	-2.02899800	-1.77040900	-0.17158200	C	-2.75437700	-0.47542400	-0.21876400
C	-1.29363600	-1.52976300	0.96809000	C	-2.74381400	-1.14982700	0.97810900
C	-1.51634000	-2.69395300	-1.14898700	C	-1.92215200	-0.89326500	-1.30625900
C	-0.04854600	-2.18869000	1.21047800	C	-1.91383200	-2.29842000	1.15980900
H	-1.67728700	-0.83380500	1.71022600	H	-3.35965000	-0.80363500	1.80434000
C	-0.33068200	-3.34680700	-0.95044700	C	-1.09649000	-1.97826700	-1.15337800
H	-2.08994600	-2.85318700	-2.05811600	H	-1.98549600	-0.36948000	-2.25644900
C	0.70310000	-1.96723600	2.37330200	C	-1.89205900	-3.01581200	2.36172200
C	0.44420800	-3.13152600	0.23197100	C	-1.06270800	-2.71966200	0.06794200
H	0.04357300	-4.04182200	-1.69834400	H	-0.46850100	-2.30484500	-1.97796900
C	1.90881100	-2.64070200	2.61513300	C	-1.07254100	-4.14020800	2.52908400
H	0.33202400	-1.26582400	3.11839200	H	-2.52846900	-2.69818500	3.18471300
C	1.64878700	-3.80288100	0.47037700	C	-0.24352500	-3.84206200	0.23485500
C	2.67749800	-2.43007900	3.80234800	C	-1.04609400	-4.88498100	3.74827000
C	2.39503700	-3.58809700	1.63749500	C	-0.22892400	-4.56767700	1.43400300
H	2.01204700	-4.51604700	-0.26687700	H	0.39346100	-4.16202700	-0.58636600
C	3.84931700	-3.10829000	4.01299400	C	-0.24016500	-5.98550400	3.87744000
H	2.30923400	-1.72191600	4.54089900	H	-1.68039700	-4.56454200	4.57043700
C	3.62058800	-4.27778200	1.89893000	C	0.59360500	-5.72280600	1.61088200
C	4.32754600	-4.04462100	3.04975600	C	0.58762400	-6.40999800	2.79653100
H	4.42102200	-2.94011200	4.92126400	H	-0.22960500	-6.54671000	4.80689900
H	3.97557900	-5.00086700	1.16821600	H	1.21741400	-6.04902400	0.78286900
H	5.25472900	-4.57794000	3.23887600	H	1.21213400	-7.28968500	2.92022500
H	-2.76585200	0.54395000	-0.89005900	H	-3.05772500	1.56818900	-0.54025700
C	-0.26370600	3.75352700	0.66802700	C	2.61177000	3.80721200	0.72552300
N	0.88910200	4.15121900	1.23691300	N	3.93705700	3.64854500	0.83538600
H	1.70343300	3.60111700	0.98738100	H	4.30956100	2.79581200	0.43290100
N	-1.43534500	4.26357600	1.09229400	N	1.99177300	4.83194300	1.33481600
H	-1.38588200	4.87327400	1.89689800	H	2.57353400	5.45040000	1.88293500
C	1.09372400	5.27770800	2.16609300	C	4.89371800	4.53177600	1.54209000
H	0.36579400	6.05194700	1.89178700	H	4.56719300	5.56456400	1.36180900
C	-2.70709200	4.32638600	0.32787000	C	0.58960400	5.26672600	1.14084700
H	-2.85529000	3.35654400	-0.15275400	H	-0.03578400	4.36524000	1.14114600
C	-2.64559800	5.41881100	-0.74673800	C	0.41387500	6.01598600	-0.18620200
H	-1.82302400	5.23892900	-1.44669200	H	0.72745700	5.40604800	-1.03984800
H	-3.57767400	5.43331600	-1.32138600	H	-0.63714400	6.28796700	-0.32841000
H	-2.50890800	6.40941100	-0.29718700	H	1.00434400	6.93825000	-0.19216500
C	-3.83890900	4.55629900	1.33089900	C	0.19061800	6.11745900	2.34905600
H	-3.88236500	3.75363500	2.07369000	H	0.29385200	5.55818100	3.28406300
H	-3.71795200	5.51354100	1.85534300	H	0.80518900	7.02400800	2.41124500
H	-4.79886200	4.59054200	0.80803400	H	-0.85081500	6.43667200	2.25375900
C	0.87224500	4.85575000	3.62602600	C	4.91762600	4.24612400	3.04969500
H	-0.12686100	4.43492200	3.78626200	H	3.92689600	4.34664100	3.50669800
H	1.60419800	4.09610100	3.92126500	H	5.27541100	3.22916200	3.24269900
H	0.98811200	5.71724000	4.29171000	H	5.59380000	4.94456300	3.55251700
C	2.49775800	5.84473300	1.93766400	C	6.27001900	4.35635900	0.89565900

H	2.63231300	6.16424700	0.89987500	H	6.24257000	4.59122400	-0.17264300
H	2.66377400	6.70728500	2.58929100	H	6.99198800	5.02323400	1.37451100
H	3.26474700	5.09743500	2.17573600	H	6.63432000	3.32963800	1.02294600
N	-0.22486400	2.83723600	-0.31301100	N	1.90202800	2.92000700	-0.00374100
C	1.01398500	2.42395500	-0.92236300	C	2.49891200	1.82166600	-0.72421400
C	1.60702000	1.23929500	-0.56136300	C	2.53619900	0.56957000	-0.15732800
C	1.59593700	3.26186300	-1.92496800	C	3.01878400	2.05246600	-2.03591000
C	2.82901700	0.82217500	-1.17607500	C	3.09959900	-0.53449800	-0.86684500
H	1.14788300	0.60316800	0.19118100	H	2.14448400	0.41246800	0.84490400
C	2.76247400	2.88764400	-2.53463000	C	3.56649000	1.01258900	-2.74094900
H	1.09232500	4.18436500	-2.19842300	H	2.97527800	3.05264900	-2.45678600
C	3.47165300	-0.36771900	-0.81306900	C	3.16627800	-1.81838400	-0.31115800
C	3.42313300	1.66801900	-2.18678700	C	3.63055600	-0.30655100	-2.19320100
H	3.20436600	3.51886000	-3.30128900	H	3.96600000	1.18274800	-3.73717800
C	4.67975700	-0.75664800	-1.40722500	C	3.74056100	-2.88876000	-1.00919100
H	3.02682300	-1.00293300	-0.05109800	H	2.77246900	-1.98847900	0.68847400
C	4.62278800	1.27222500	-2.78824600	C	4.19553800	-1.37896300	-2.89341400
C	5.35503700	-1.96054900	-1.03436300	C	3.83212400	-4.20056600	-0.44753700
C	5.26845200	0.08260700	-2.42662600	C	4.26688400	-2.66352500	-2.33806400
H	5.06754200	1.90571000	-3.55260300	H	4.59620200	-1.20989200	-3.89016000
C	6.53340000	-2.31641600	-1.63570500	C	4.40375400	-5.22538200	-1.15543000
H	4.91755500	-2.58214400	-0.25753400	H	3.45063000	-4.36575900	0.55696500
C	6.49737700	-0.32877100	-3.02942700	C	4.85118700	-3.76218100	-3.04127300
C	7.11008500	-1.49266000	-2.64685500	C	4.91707400	-5.00455400	-2.46781800
H	7.03979800	-3.23196700	-1.34347700	H	4.47828400	-6.21632700	-0.71708800
H	6.93719800	0.30216900	-3.79758800	H	5.24734800	-3.59173400	-4.03864300
H	8.04418400	-1.79488300	-3.11157500	H	5.36735200	-5.83124700	-3.00885900
H	-1.08324000	2.31481300	-0.57668800	H	0.88627300	2.98125200	-0.02756700
O	-2.43666700	1.42358700	-1.25652400	O	-0.87477100	2.17238900	-0.84623500
H	-2.26028600	1.24082700	-2.19245800	H	-0.61908700	1.23202500	-0.80228700
				H	-0.73856000	2.40487100	-1.78008400

Spectral equipment and measurements.

UV-Vis absorption spectra were acquired at 298 K on a V-750 spectrophotometer (JASCO) using a slit width of 0.4 nm and a scan rate of 600 nm min^{-1}. Steady-state fluorescence (SSF) spectra were recorded on an FLS920 spectrofluorometer (Edinburgh Instruments) equipped with an MCP-PMT (microchannel plate-photomultiplier tube) detector (R3809 model) and a TCSPC (time-correlated single photon counting) data acquisition card (TCC900 model). A Xe lamp of 450 W was used as the light source for SSF spectra and a sub-nanosecond pulsed Light-Emitting Diode, EPLED-360 (Edinburgh Photonics), was employed as a light source at 368 nm for Time-resolved fluorescence decays (TRF). A TLC 50 temperature-controlled cuvette holder (Quantum Northwest) was used to keep the temperature at 298 K during the spectra acquisition. The measurement properties such as excitation and emission wavelength (λ_{ex} and λ_{em}), excitation and emission slits ($\Delta\lambda_{ex}$ and $\Delta\lambda_{em}$), the step and dwell time were different for each experiment and they are indicated in the related experiment, table or figure. All measurements were performed using a 10 mm quartz cuvette (Hellma Analytics)

The fluorescence intensity decay, *I(t)*, was fitted to the following multiexponential function using an iterative least-squares fit method

$$I(t) = \sum_{i=1}^{n} \alpha_i exp(-t/\tau_i) \quad (1)$$

where α_i and τ_i are the amplitude and lifetime for each *i*th term. The mean lifetime of the decay was then calculated as:

$$\tau_m = \frac{\sum_{i=1}^{n} \alpha_i \tau_i^2}{\sum_{i=1}^{n} \alpha_i \tau_i} \quad (2)$$

Solutions of 1GA (10 μM) were prepared in different solvents from stock solutions (1 mM) of 1GA in the same solvent. For experiments in water, stock solutions of 1GA (1 mM) in ethanol were used. For the pH titration experiments, an aqueous solution (10 μM) was titrated by the successive addition of small volumes (in the order of microliters) of HCl and NaOH solutions of different concentrations (0.01–10 M) to an initial volume of 25 mL in order to minimize changes in the sample. SSF (λ_{ex} 368 nm, $\Delta\lambda_{ex}$ and $\Delta\lambda_{em}$ 3 nm, step 1 nm and 0.1s dwell time) and TRF (λ_{ex} 368 nm, λ_{em} 510 nm, $\Delta\lambda_{ex}$ 0.1 nm and $\Delta\lambda_{em}$ 10 nm) spectra of 1GA were recorded.

On the other hand, the titration with trifluoroacetic acid (TFA) was done using solutions of 1GA (10 μM) in acetonitrile to which small volumes of [1GA] : [TFA] mixtures with a mixing ratio varying from 0 to 100) were added. For these solutions the fluorescence decays were recorded under following conditions: λ_{ex} 368 nm, λ_{em} 492 nm, $\Delta\lambda_{ex}$ 0.1 nm and $\Delta\lambda_{em}$ 10 nm.

For the solutions with different 1GA concentrations (varying from 1 μM to 1 mM) the fluorescence decays recorded under following conditionsλ_{ex} 360 nm, λ_{em} 495 nm. Also the fluorescence decay of time-resolved fluorescence spectrum (λ_{ex} 368 nm, λ_{em} 492 nm, $\Delta\lambda_{ex}$ 0.1 nm and $\Delta\lambda_{em}$ 10 nm) of a solution of 1GA (10 μM) in deuterated water was recorded.

Time-resolve fluorescence decays (λ_{ex} 368 nm, λ_{em} 504 nm, $\Delta\lambda_{ex}$ 0.1 nm and $\Delta\lambda_{em}$ 10 nm) of solutions of 1GA (10 μM) in acetonitrile / H_2O, from 0 to 1, were acquired.

The quantum yield was calculated using an integrated sphere as described elsewhere.[4]

Table S2. Average fluorescence lifetime of 1GA in acetonitrile at different concentrations of TFA. Standard deviation of 15% is included.

[Acetonitrile] : [TFA]	**τ_m (ns)**
1 : 0	11.20±1.67
1 : 1	11.10±1.65
1 : 10	11.05±1.65

1 : 50	10.98±1.65
1 : 100	10.92±1.63

Table S3. Partial (τ_i) and average (τ_m) fluorescence lifetime of 1GA from Figure 2 of the manuscript.

	τ_1 / ns	α_1	τ_2 / ns	α_2	τ_3 / ns	α_3	τ_m / ns
pH 2.1	25.1	5.09×10^{-1}					25.0
pH 3.9	24.4	1.28×10^{5}	41.3	3.24×10^{-3}			25.1
pH 6.0	24.6	7.86×10^{-3}					24.6
pH 7.0	0.22	1.35×10^{-2}	9.63	4.00×10^{-4}	25.10	7.34×10^{-3}	24.4
pH 8.0	0.27	1.29×10^{-2}	7.57	4.49×10^{-4}	25.10	8.06×10^{-3}	24.4
pH 10.2	0.89	2.51×10^{-3}	24.9	7.83×10^{-3}			24.6
pH 11.8	0.66	6.72×10^{-2}	14.1	1.25×10^{-1}	44.60	2.30×10^{-4}	14.0
D_2O	0.00	1.91×10^{-1}	7.64	4.09×10^{-3}	30.80	5.87×10^{-2}	30.4
H_2O	0.13	6.03×10^{-3}	24.7	1.86×10^{-2}			24.6
χ_{H2O} 0	1.55	1.98×10^{-3}	11.3	2.41×10^{-2}			11.2
χ_{H2O} 0.24	1.49	1.44×10^{-3}	14.1	1.46×10^{-2}			14.0
χ_{H2O} 0.42	1.38	1.71×10^{-3}	16.3	1.55×10^{-2}			16.1
χ_{H2O} 0.55	2.28	8.90×10^{-4}	18.2	1.40×10^{-2}			18.1
χ_{H2O} 0.65	4.33	9.67×10^{-4}	20.5	1.73×10^{-2}			20.3
χ_{H2O} 0.74	1.67	1.63×10^{-3}	22.5	2.47×10^{-2}			22.4
χ_{H2O} 0.81	5.14	3.71×10^{-4}	24.6	1.12×10^{-2}			24.5
χ_{H2O} 0.87	3.09	4.41×10^{-4}	25.9	1.59×10^{-2}			25.8
χ_{H2O} 0.91	0.84	8.86×10^{-4}	26.2	1.44×10^{-2}			26.1
χ_{H2O} 0.96	2.77	2.41×10^{-4}	25.8	1.36×10^{-2}			25.8
χ_{H2O} 1.00	5.89	2.11×10^{-5}	24.7	8.50×10^{-3}			24.7
pH 7.0 (1µM)	0.07	-3.60×10^{-3}	3.51	9.61×10^{-3}	22.00	5.36×10^{-2}	21.5
pH 7.0 (10µM)	0.07	2.39×10^{-2}	3.51	1.59×10^{-2}	22.00	2.47×10^{-2}	20.2
pH 7.0 (100µM)	0.07	1.05×10^{-01}	3.51	1.07×10^{-2}	22.00	8.00×10^{-3}	18.10
pH 7.0 (1000µM)	0.07	9.30×10^{-02}	3.51	3.66×10^{-2}	22.00	8.40×10^{-2}	14.10

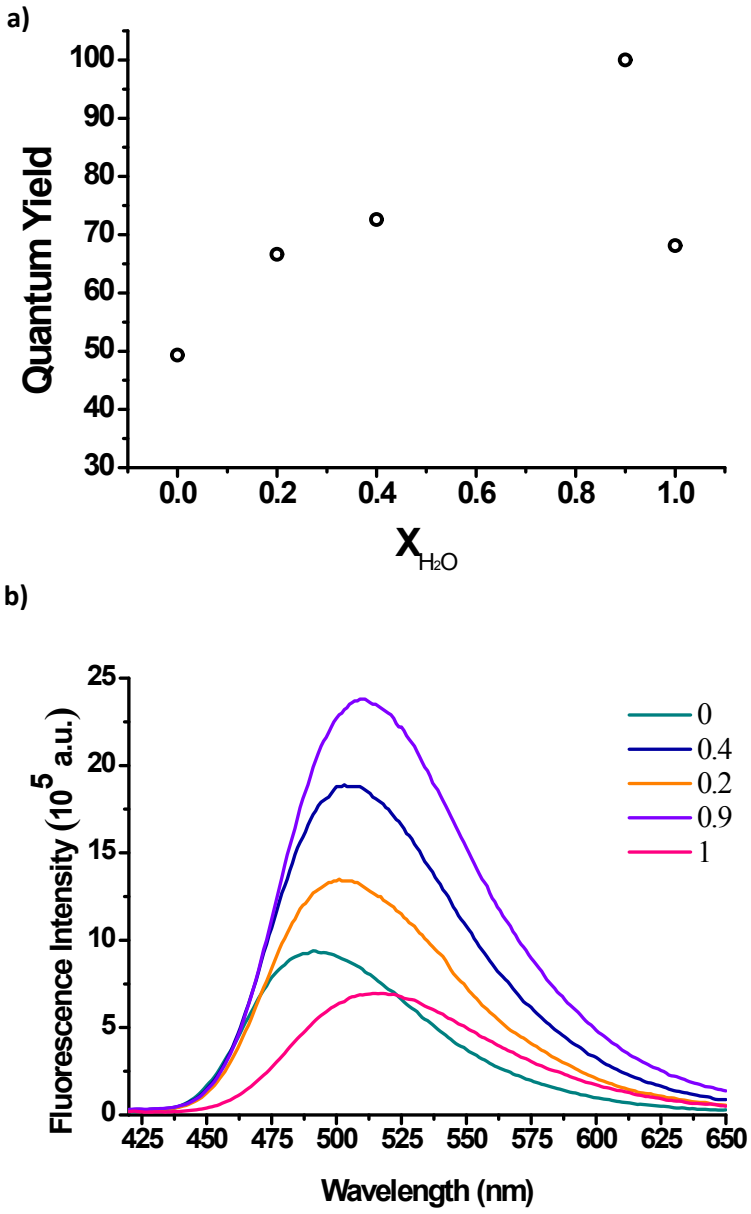

Figure 2S. a) Quantum Yield of 1GA in ACN in presence of varying water content; b) Emission spectra of 1GA in ACN in presence of varying water content. Molar fraction (χH_2O). λ_{exc} = 360 nm

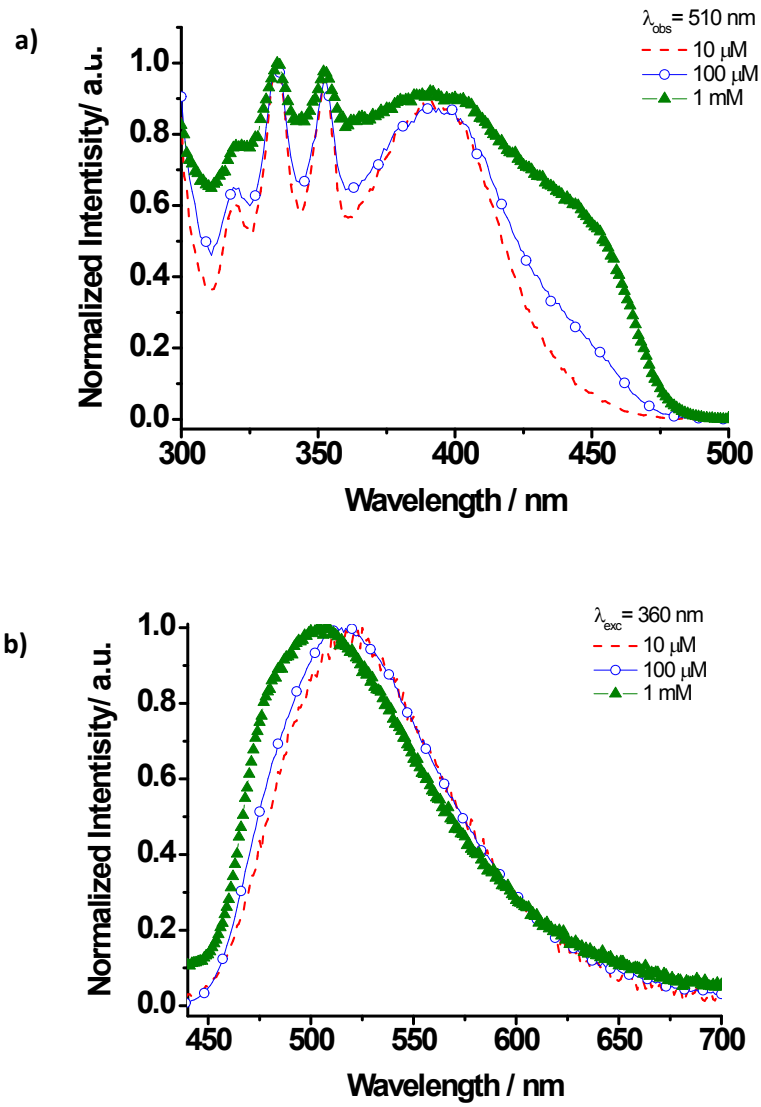

Figure 3S. Concentration dependence of the excitation (a) and emission (b) spectra of 1GA in aqueous solution, pH 7. λ_{em} = 510 nm and λ_{exc} = 360 nm

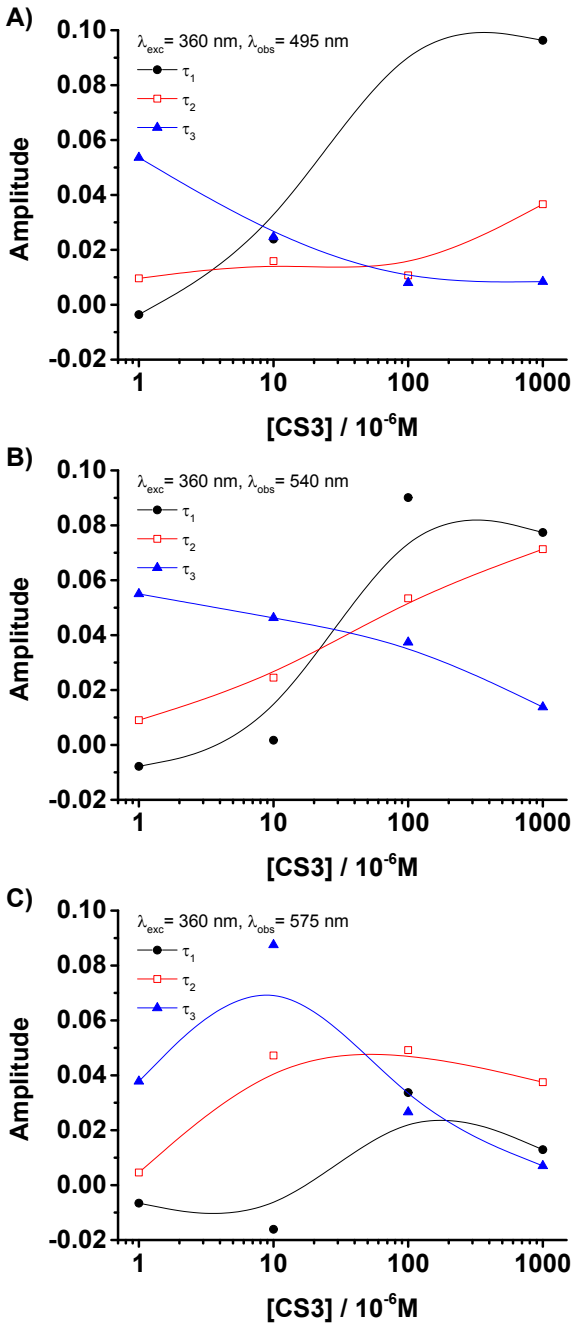

Figure 4S. Concentration dependence of the obtained lifetime amplitudes observed at 495 nm (A), 540 nm (B) and 575 nm (C).

SAXS experiments. SAXS experiments have been conducted at the Dutch-Belgian Beamline (DUBBLE) station BM26B of the European Synchrotron Radiation Facility (ESRF) in Grenoble (France).[5,6] The samples were prepared by drop-casting method from a water solution of 1mM 1GA in a mica sheet. The distance between the SAXS detector and the sample was set to ca. 2417.81 mm using a wavelength of 0.979 Å. The 2D SAXS patterns were collected in a Dectris-Pilatus 1M detector with a resolution of 981×1043 pixels and a pixel size of 172 × 172 μm. The scattering data was been reduced using the Bubble server integrator version 1.11-20181129.140754. The data integration has considered the standard corrections for sample absorption and background subtraction as well as normalized to the intensity of the incident beam to correct for primary beam intensity fluctuations. The scattering pattern of AgBe has been employed to calibrate the wavevector scale of the scattering profile. WAXS patterns were recorded by a Pilatus 300 K-W (linear configuration, 254mm x 33.5mm active area) fitted with a pixel size of 172 μm2. The calibration of the wavenumber $q = 4\pi/\lambda \sin\theta$ scale for WAXS measurements has been completed using the scattering pattern of alpha-alumina as standard.

The data fitting was conducted using the MINUITS minimization program developed by the CERN[5,6] to obtain quantitative information about the structure of the clusters in the film using a model of non interacting spheres (see equation) to adjust the experimental SAXS measured 1D profile intensity (I(q)) (3):

$$I(q) = \frac{scale}{V}\left[\frac{3V(\Delta\rho)\sin(qr) - qr\cos(qr))}{(qr)^3}\right]_2 \quad (3)$$

Interestingly, the scattering of the film produced by drop-casting have shown the presence of spherical-like aggregates of mostly ca 0.6 nm of a radius in the high q region whilst the scattering at low q angles suggest the coexistence of negligible content of spherical cluster of ca 9.29 nm of the radius (see Figure 5Sa). Moreover, The WAXS confirms that the film possesses an amorphous arrangement generated by the presence of water. However, the presence of diffraction reflections superposed on the amorphous hallo suggested that aggregates maintain the internal order of the solid compound (see Figure 5Sb).

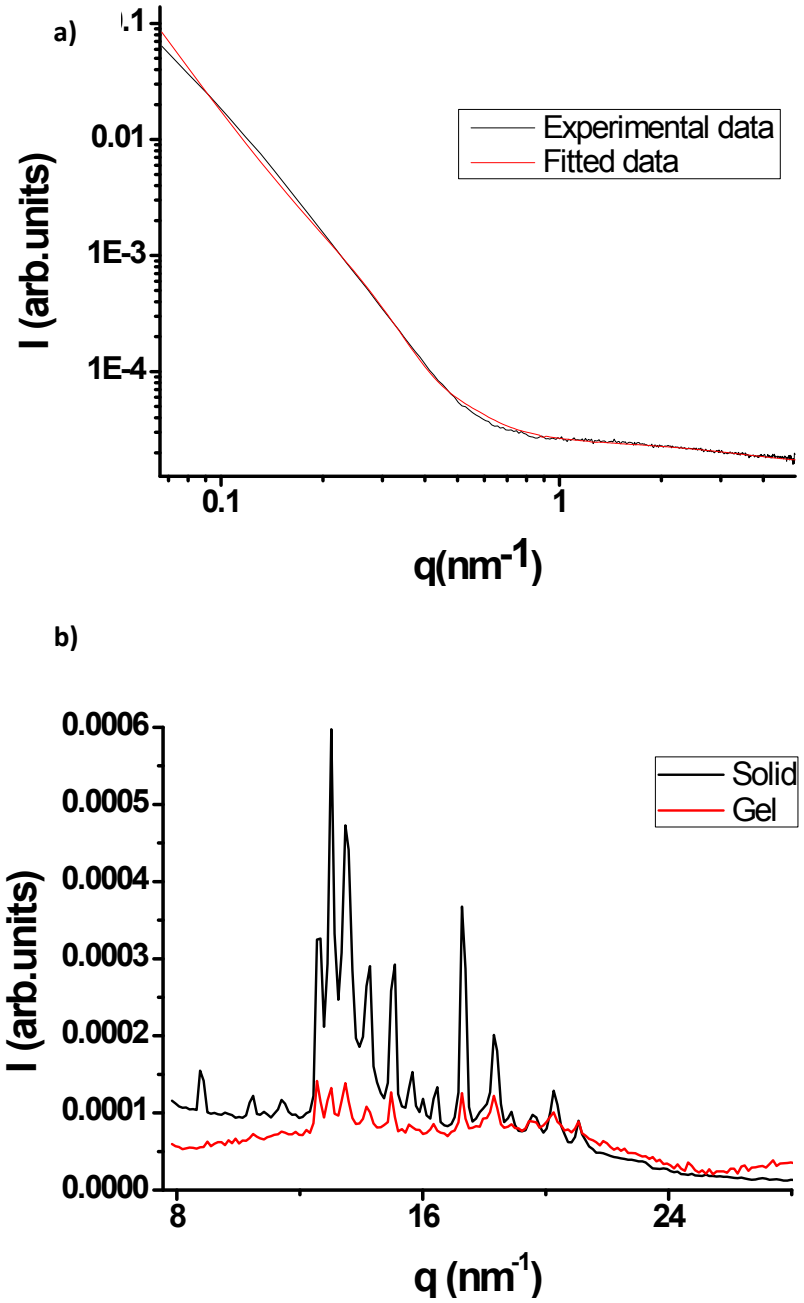

Figure 5S. a) SAXS profiles of drop cast of 1GA; b) WAXS profiles of drop cast of 1GA 10^{-5} M.

Synthesis and Characterization of 1GA. Synthesis reactions were performed using standard Schlenk and glove-box techniques under an atmosphere of dry nitrogen. Solvents were purified by passage through a column of activated alumina (Innovative Tech.), degassed under nitrogen and stored over molecular sieves in the glove box prior to use..
In a glovebox, 0.04 mL of a solution of $ZnEt_2$ in hexane (1M) was added to a solution of 1-aminoanthracene (2 mmol) in dry THF (20 mL) in a Schlenk tube. *N,N'*-diisopropylcarbodiimide (2 mmol) was then added to the above reaction mixture. The Schlenk tube was taken outside the glovebox, and the reaction was carried out at 50 °C for 3 h. The solution was concentrated under reduced pressure, hexane was added and the mixture was placed in a refrigerator at -30 °C for 16 h. After filtration the guanidine products were obtained as white microcrystalline solids in 95% yield. M. p. 257-258°C. HRMS (ESI+): calcd. m/z 321.21 [M+H]+; found: 321.21 IR Neat: νmax 3400, 1634 (C=N), 1215, 1182 (C-N), 1460, 1315, 954, 884, 736 cm-1.

NMR characterization. All NMR experiments were conducted in acetonitrile-d_3 at 298 K in a Bruker Avance II 600 MHz spectrometer equipped with a 5-mm triple-nucleus (TXI) probe head with z-gradient coil with a maximum gradient strength of 50 G/cm-1. The ^1H π/2 pulse length was adjusted for each sample. Typical ^1H, ^{13}C and bidimensional NMR experiments (NOESY, COSY, HSQC and HMBC) from the Bruker pulse program pulse list were used for full NMR characterization of 1GA. The standard Bruker pulse program 'ledbpgp2s' was used for diffusion measurement and 128 scans with 65k data points were acquired. Gradients were incremented in 11 steps from 2.408 G cm^{-1} to 45.743G cm^{-1}, using an exponential ramp. Gradient pulse (δ) was set to 0.5ms, diffusion time (Δ) was set to 50 ms, eddy current delay was set to 5.0 ms and delay for gradient recovery was set to 0.2 ms. All spectra were processed by TopSpin 3.2 software supplied by Bruker. Line broadening Lorentzian function of 1 Hz was applied, and dimension and each row were phased and baseline corrected before Fourier transformation execution in F2 dimension.

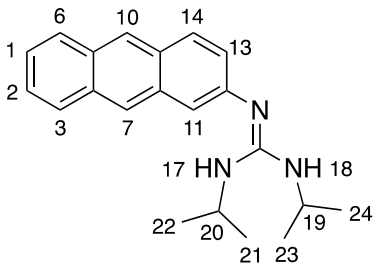

^{1}H NMR (600 MHz, Acetonitrile-d_3) δ 8.29 (s, 1H, **H_{10}**), 8.08 (s, 1H, **H_7**), 7.92 (d, J = 8.5 Hz, 1H, **H_3**), 7.88 (d, J = 8.5 Hz, 1H, **H_6**), 7.84 (d, J = 9.0 Hz, 1H, **H_{14}**), 7.39 (t, J = 7.3 Hz, 1H, **H_1**), 7.32 (t, J = 7.5 Hz, 1H, **H_2**), 7.04 (d, J = 8.9 Hz, 1H, **H_{13}**), 7.00 (s, 1H, **H_{11}**), 4.50 (s, 2H, **NH**), 3.72 (hept, J = 13.3, 6.6, 6.2 Hz, 2H, **H_{20}, H_{19}**), 1.05 (d, J = 6.5 Hz, 12H, **H_{21}, H_{22}, H_{23}, H_{24}**).

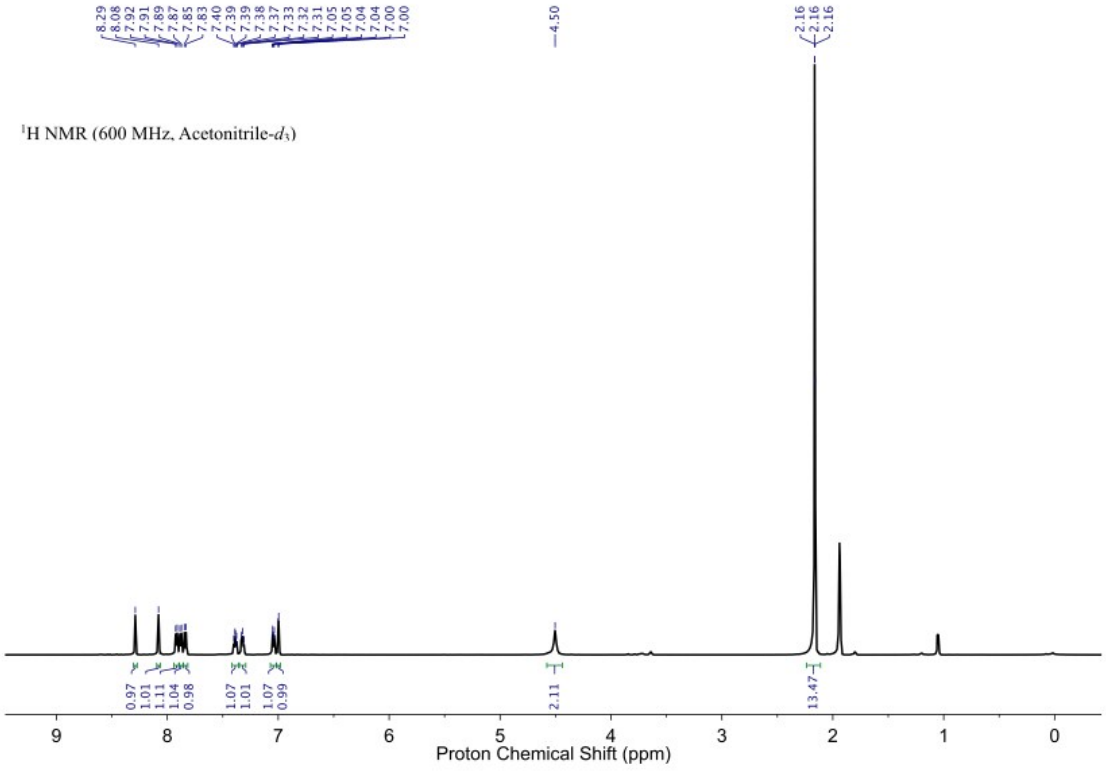

Figure 6S. 1H NMR spectrum.

^{13}C NMR (151 MHz, CD_3CN) δ 146.2902 (**C_{12}**, **C_{16}**), 134.7335 (**C_4, C9**), 133.3608 (**C_5, C_8**), 130.2745 (**C_{14}**), 129.1230 (**C_6**), 128.2025 (**C_3**), 126.9885 (**C_{10}**), 126.3091 (**C_1**), 124.5481 (**C_2**), 122.8265 (**C_7**), 121.4478 (**C_{13}**), 105.1888 (**C_{11}**), 42.4388 (**C_{19}, C_{20}**), 23.5020 (**C_{21}, C_{22}, C_{23}, C_{24}**).

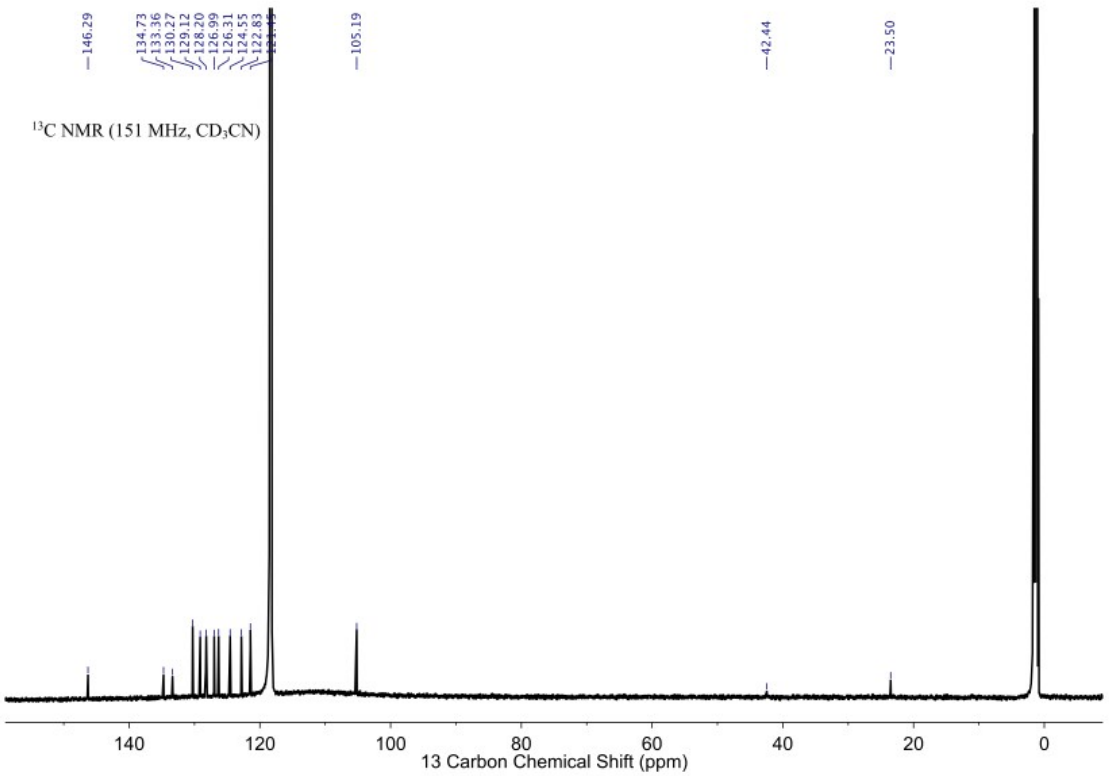

Figure 7S. ^{13}C NMR spectrum.

COSY correlation:

^{1}H NMR (600 MHz, CD_3CN) δ 8.5371, 8.2892, 8.0421, 8.3273, 8.0795, 7.8326, 7.9185, 7.3227, 7.8742, 7.3883, 7.8358, 7.0455, 7.8384, 7.3920, 7.8801, 7.9193, 7.3240, 7.0459, 7.8393, 7.2463, 6.9978, 6.7508, 4.5047, 3.8460, 3.7862, 3.7423, 3.6407, 2.4120, 2.1641, 1.9177, 1.8080, 2.1860, 1.9398, 1.6930, 1.5841, 1.7944, 1.2644, 1.2010, 3.7211, 1.0525, 0.0746, 0.0163

^{1}H NMR (600 MHz, CD_3CN) δ 8.2904, 8.2901, 8.2879, 8.0824, 8.0808, 8.0790, 7.9261, 7.9190, 7.8828, 7.8791, 7.8487, 7.8388, 7.8253, 7.3922, 7.3845, 7.3261, 7.3228, 7.0551, 7.0444, 6.9993, 6.9990, 6.9990, 4.5054, 3.8466, 3.7851, 3.7507, 3.6413, 2.1645, 2.1642, 2.1642, 2.1636, 1.9441, 1.9403, 1.9402, 1.9395, 1.7995, 1.2656, 1.2007, 1.0537, 1.0530, 0.0805, 0.0179.

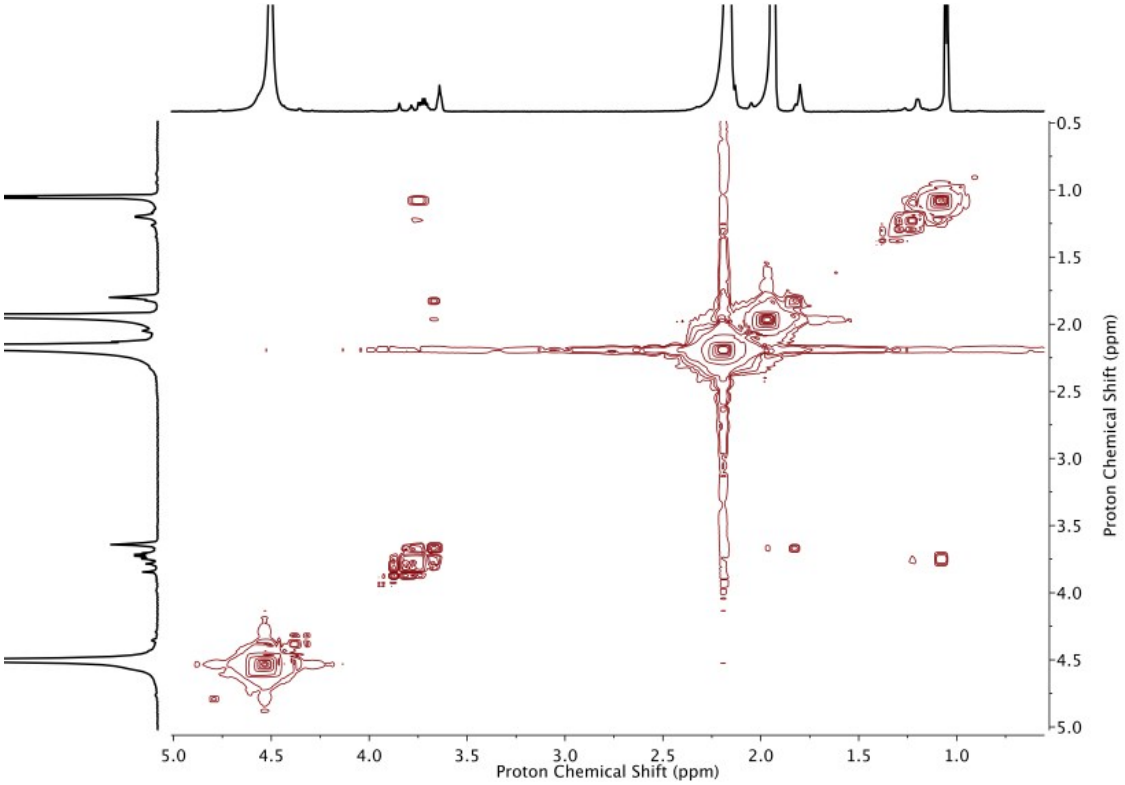

Figure 8S. COSY spectrum.

HSQC correlations:

^{13}C NMR (151 MHz, CD_3CN) δ 126.8397, 122.6871, 128.9687, 128.0724, 130.1273, 126.1525, 124.3948, 121.2987, 105.0510, 42.1968, 1.7473, 26.1465, 22.9136, 23.3722

^{1}H NMR (600 MHz, CD_3CN) δ 8.2894, 8.0824, 7.9187, 7.8824, 7.8397, 7.3901, 7.3247, 7.0500, 7.0007, 3.7213, 1.9048, 1.7998, 1.2032, 1.0568.

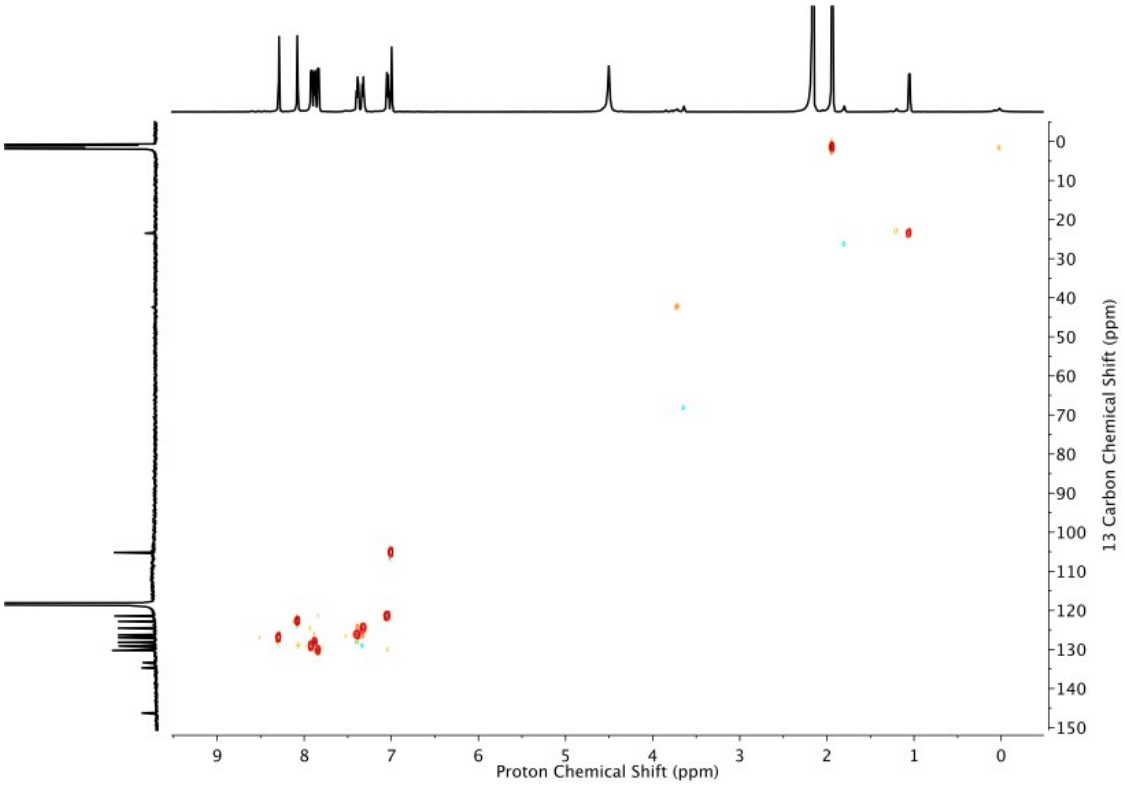

Figure 9S. HSQC spectrum.

HMBC correlations:

^{13}C NMR (151 MHz, CD_3CN) δ 129.7528, 133.9307, 129.6610, 129.6614, 133.9239, 128.2382, 105.1758, 128.2122, 105.1885, 105.2072, 128.2731, 126.4456, 133.4115, 133.3011, 126.4491, 133.3545, 126.7187, 124.4056, 130.2214, 122.9986, 130.2302, 124.5096, 122.9311, 130.1679, 124.5188, 146.2852, 134.7342, 127.1109, 127.1917, 146.3018, 134.7459, 127.1342, 136.7795, 127.0732, 146.1940, 133.4298, 129.1782, 129.0861, 133.3742, 133.3653, 129.1282, 129.1159, 133.3613, 128.3260, 130.2482, 128.2414, 105.1457, 128.2943, 128.2720, 105.1743, 105.1340, 128.2188, 121.7484, 128.2526, 121.8199, 128.2687, 121.9422, 118.3219, 118.3156, 120.3713, 118.3211, 120.4027, 118.3313, 23.4623, 42.3716, 23.4599, 42.3835, 44.4655, 42.4113, 23.4624, 25.5377, 44.4984, 42.3924, 23.3960

^{1}H NMR (600 MHz, CD_3CN) δ 8.3012, 8.2887, 8.2884, 8.2789, 8.2770, 8.0826, 8.0825, 8.0708, 8.0708, 8.0619, 8.0615, 7.9286, 7.9268, 7.9143, 7.9126, 7.8994, 7.8986, 7.8922, 7.8900, 7.8899, 7.8781, 7.8770, 7.8633, 7.8631, 7.8600, 7.8457, 7.8425, 7.8422, 7.8341, 7.8281, 7.8245, 7.8242, 7.8237, 7.8159, 7.8106, 7.4072, 7.4039, 7.3918, 7.3914, 7.3780, 7.3779, 7.3649, 7.3639, 7.3318, 7.3185, 7.3044, 7.0547, 7.0542, 7.0381, 7.0380, 7.0243, 7.0212, 7.0026, 7.0026, 6.9901, 6.9901, 6.9776, 1.9522, 1.9398, 1.9393, 1.9252, 1.9237, 1.9140, 1.0611, 1.0609, 1.0522, 1.0522, 1.0522, 1.0414, 1.0413, 1.0411, 1.0411, 1.0331, 1.0329.

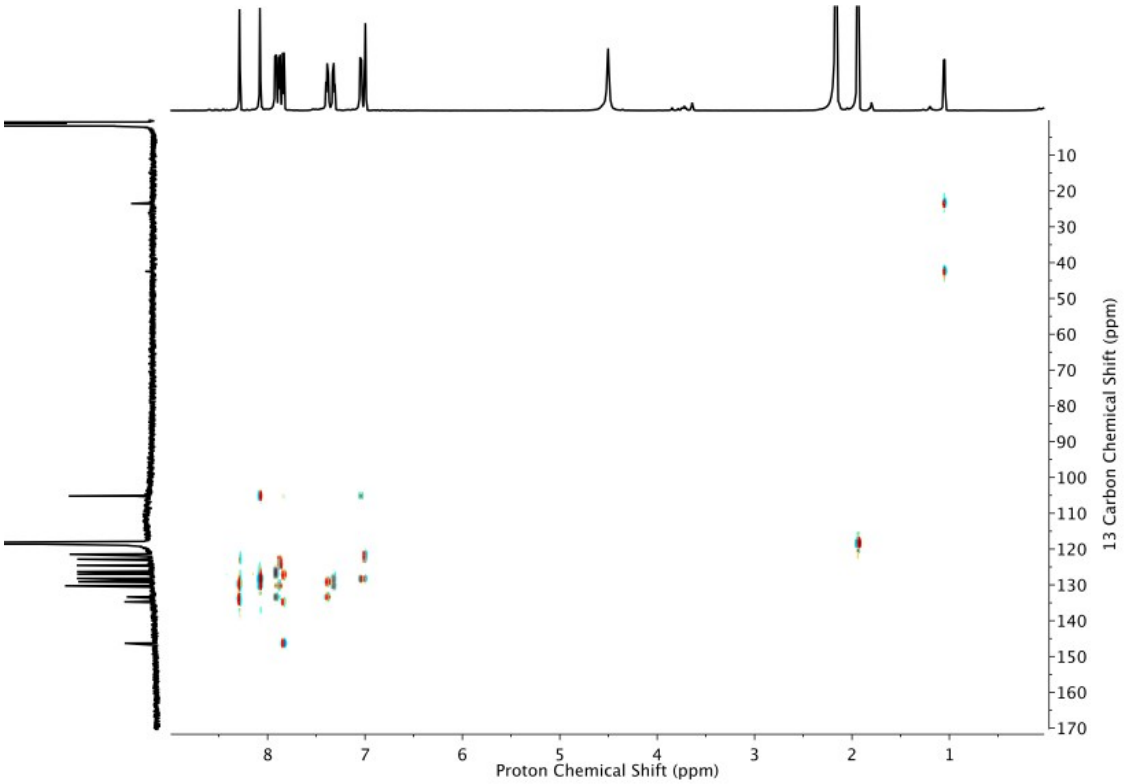

Figure 10S. HMBC spectrum.

REFERENCES

(1) Frisch, M. J.; Trucks, G. W.; Schlegel, H. B.; Scuseria, G. E.; Robb, M. A.; Cheeseman, J. R.; Scalmani, G.; Barone, V.; Petersson, G. A.; Nakatsuji, H.; Li, X.; Caricato, M.; Marenich, A. V.; Bloino, J.; Janesko, B. G.; Gomperts, R.; Mennucci, B.; Hratchian, H. P.; Ortiz, J. V.; Izmaylov, A. F.; Sonnenberg, J. L.; Williams; Ding, F.; Lipparini, F.; Egidi, F.; Goings, J.; Peng, B.; Petrone, A.; Henderson, T.; Ranasinghe, D.; Zakrzewski, V. G.; Gao, J.; Rega, N.; Zheng, G.; Liang, W.; Hada, M.; Ehara, M.; Toyota, K.; Fukuda, R.; Hasegawa, J.; Ishida, M.; Nakajima, T.; Honda, Y.; Kitao, O.; Nakai, H.; Vreven, T.; Throssell, K.; Montgomery Jr., J. A.; Peralta, J. E.; Ogliaro, F.; Bearpark, M. J.; Heyd, J. J.; Brothers, E. N.; Kudin, K. N.; Staroverov, V. N.; Keith, T. A.; Kobayashi, R.; Normand, J.; Raghavachari, K.; Rendell, A. P.; Burant, J. C.; Iyengar, S. S.; Tomasi, J.; Cossi, M.; Millam, J. M.; Klene, M.; Adamo, C.; Cammi, R.; Ochterski, J. W.; Martin, R. L.; Morokuma, K.; Farkas, O.; Foresman, J. B.; Fox, D. J. Wallingford, CT, 2016.

(2) Longo, A.; Calandra, P.; Casaletto, M.; Giordano, C.; Venezia, A.; Liveri, V. T. Synthesis and Physico-Chemical Characterization of Gold Nanoparticles Softly Coated by Aot *Mater. Chem. Phys.* **2006**, *96*, 66-72.

(3) Tomasi, J.; Mennucci, B.; Cammi, R. Quantum Mechanical Continuum Solvation Models *Chem. Rev.* **2005**, *105*, 2999-3094.

(4) Coutino-Gonzalez, E.; Roeffaers, M. B. J.; Dieu, B.; De Cremer, G.; Leyre, S.; Hanselaer, P.; Fyen, W.; Sels, B.; Hofkens, J. Determination and Optimization of the Luminescence External Quantum Efficiency of Silver-Clusters Zeolite Composites *J. Phys. Chem. C* **2013**, *117*, 6998-7004.

(5) Portale, G.; Cavallo, D.; Alfonso, G. C.; Hermida-Merino, D.; Drongelen, M. v.; Balzano, L.; Peters, G.; Goossens, J.; Bras, W. Polymer Crystallization Studies under Processing-Relevant Conditions at the Saxs/Waxs Dubble Beamline at the Esrf *J. Appl. Crystallogr.* **2013**, *46*, 1681-89.

(6) Bras, W.; Dolbnya, I. P.; Detollenaere, D.; Van Tol, R.; Malfois, M.; Greaves, G. N.; Ryan, A. J.; Heeley, E. Recent Experiments on a Small-Angle/Wide-Angle X-Ray Scattering Beam Line at the Esrf *J. Appl. Crystallogr.* **2003**, *36*, 791-94.